

Constant-Time Predictive Distributions for Gaussian Processes

Geoff Pleiss¹ Jacob R. Gardner¹ Kilian Q. Weinberger¹ Andrew Gordon Wilson¹

Abstract

One of the most compelling features of Gaussian process (GP) regression is its ability to provide well calibrated posterior distributions. Recent advances in inducing point methods have drastically sped up marginal likelihood and posterior mean computations, leaving posterior covariance estimation and sampling as the remaining computational bottlenecks. In this paper we address this shortcoming by using the Lanczos decomposition algorithm to rapidly approximate the predictive covariance matrix. Our approach, which we refer to as LOVE (Lanczos Variance Estimates), substantially reduces the time and space complexity over any previous method. In practice, it can compute predictive covariances up to 2,000 times faster and draw samples 18,000 time faster than existing methods, all *without* sacrificing accuracy.

1. Introduction

Gaussian processes (GPs) are fully probabilistic models which can naturally estimate predictive uncertainty through posterior variances. These uncertainties play a pivotal role in many application domains. For example, uncertainty information is crucial when incorrect predictions could have catastrophic consequences, such as in medicine (Schulam & Saria, 2017) or large-scale robotics (Deisenroth et al., 2015); Bayesian optimization approaches typically incorporate model uncertainty when choosing actions (Snoek et al., 2012; Deisenroth & Rasmussen, 2011; Wang & Jegelka, 2017); and reliable uncertainty estimates are arguably useful for establishing trust in predictive models, especially when predictions would be otherwise difficult to interpret (Doshi-Velez & Kim, 2017; Zhou et al., 2017).

Although predictive uncertainties are a primary advantage of GP models, they have recently become their primary computational bottleneck. Historically, this has not always been the case. The use of GPs used to be limited to problems with

¹Cornell University. Correspondence to: Geoff Pleiss <geoff@cs.cornell.edu>, Jacob R. Gardner <jrg365@cornell.edu>, Andrew Gordon Wilson <andrew@cornell.edu>.

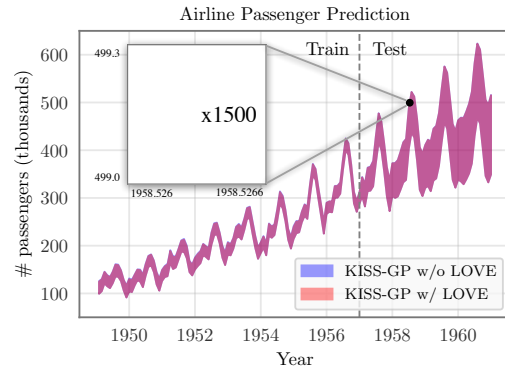


Figure 1. Comparison of predictive variances on airline passenger extrapolation. The variances predicted with LOVE are accurate within 10^{-4} , yet can be computed orders of magnitude faster.

small datasets, since learning and inference computations naïvely scale cubically with the number of data points (n). However, recent advances in *inducing point methods* have managed to scale up GPs to much larger datasets (Snelson & Ghahramani, 2006; Quiñero-Candela & Rasmussen, 2005; Titsias, 2009). For example, *Kernel Interpolation for Scalable Structured GPs* (KISS-GP) scales to millions of data points (Wilson & Nickisch, 2015; Wilson et al., 2015). For a given test point \mathbf{x}^* , KISS-GP expresses the GP’s predictive mean as $\mathbf{a}^\top \mathbf{w}(\mathbf{x}^*)$, where \mathbf{a} is a pre-computed vector dependent only on training data, and $\mathbf{w}(\mathbf{x}^*)$ is a sparse interpolation vector. This particular formulation affords the ability to compute predictive means in *constant time*, independent of n .

However, these computational savings do not extend naturally to predictive uncertainties. With KISS-GP, computing the predictive covariance between two test points requires $\mathcal{O}(n + m \log m)$ computations, where m is the number of inducing points used (see Table 1). While this asymptotic complexity is lower than that of standard Gaussian process inference, it quickly becomes prohibitive when n is large, or when we wish to make many repeated computations. Additionally, drawing samples from the predictive distributions – a necessary operation in many applications – is similarly expensive. Matching the reduced complexity of predictive mean inference has remained an open problem.

In this paper, we provide a solution based on the tridi-

agonalization algorithm of Lanczos (1950). Our method takes inspiration from KISS-GP’s mean computations: we express the predictive covariance between \mathbf{x}_i^* and \mathbf{x}_j^* as $\mathbf{w}(\mathbf{x}_i^*)^\top \mathbf{C} \mathbf{w}(\mathbf{x}_j^*)$, where \mathbf{C} is an $m \times m$ matrix dependent only on training data. However, crucially, we take advantage of the fact that \mathbf{C} affords fast matrix-vector multiplications (MVMs) to avoid explicitly computing the matrix. Using the Lanczos algorithm, we can efficiently decompose \mathbf{C} as two rank- k matrices $\mathbf{C} \approx \mathbf{R}^\top \mathbf{R}'$ in *nearly linear time* – $\mathcal{O}(kn + km \log m)$. After this one-time upfront computation, and due to the special structure of \mathbf{R}, \mathbf{R}' , all variances can be computed in *constant time* – $\mathcal{O}(k)$ per (co)variance entry. Further, we extend our method to sample from the predictive distribution at t points in $\mathcal{O}(t + m)$ time – independent of training dataset size.

We refer to this method as LanczOs Variance Estimates, or LOVE for short. LOVE has the lowest asymptotic complexity of any method for computing predictive (co)variances and drawing samples with GPs. We empirically validate LOVE on seven datasets and find that it *consistently* provides substantial speedups over existing methods: Variances and samples are accurate to within four decimals, and can be computed *up to 18,000 times faster*.

2. Background

A Gaussian process is a prior over functions *functions*, $p(f(\mathbf{x}))$, specified by a *prior mean function* $\mu(\mathbf{x})$ and *prior covariance function* $k(\mathbf{x}, \mathbf{x}')$. Given a dataset of observations $\mathcal{D} = (X, \mathbf{y}) = \{(\mathbf{x}_i, y_i)\}_{i=1}^n$ and a Gaussian noise model, the posterior $p(f(\mathbf{x}) | \mathcal{D})$ is again a Gaussian process with mean $\mu_{f|\mathcal{D}}(\mathbf{x}^*)$ and covariance $k_{f|\mathcal{D}}(\mathbf{x}^*, \mathbf{x}'^*)$:

$$\mu_{f|\mathcal{D}}(\mathbf{x}^*) = \mu(\mathbf{x}^*) + \mathbf{k}_{X\mathbf{x}^*}^\top \widehat{K}_{XX}^{-1} (\mathbf{y} - \mu(X)), \quad (1)$$

$$k_{f|\mathcal{D}}(\mathbf{x}^*, \mathbf{x}'^*) = k_{\mathbf{x}^* \mathbf{x}'^*} - \mathbf{k}_{X\mathbf{x}^*}^\top \widehat{K}_{XX}^{-1} \mathbf{k}_{X\mathbf{x}'^*}, \quad (2)$$

where K_{AB} denotes the kernel matrix between A and B , $\widehat{K}_{XX} = K_{XX} + \sigma^2 I$ (for observed noise σ) and $\mathbf{y} = [y(\mathbf{x}_1), \dots, y(\mathbf{x}_n)]^\top$. Given a set of t test points X^* , the equations above give rise to a t dimensional multivariate Gaussian joint distribution $p([f(\mathbf{x}_1^*), \dots, f(\mathbf{x}_t^*)] | \mathcal{D})$ over the function values of the t test points. This last property allows for sampling functions from a posterior Gaussian process by sampling from this joint predictive distribution. For a full overview, see (Rasmussen & Williams, 2006).

2.1. Inference with matrix-vector multiplies

Computing predictive means and variances with (1) and (2) requires computing solves with the kernel matrix \widehat{K}_{XX} (e.g. $\widehat{K}_{XX} \mathbf{y}$). Linear solves for GPs are often computed using the Cholesky decomposition of $\widehat{K}_{XX} = LL^\top$, which requires $\mathcal{O}(n^3)$ time to compute. Linear conjugate gradients (linear CG) provides an alternative approach that

solves linear systems through only matrix-vector multiplies (MVMs) with \widehat{K}_{XX} . Linear CG exploits the fact that the solution $A^{-1} \mathbf{b}$ is the unique minimizer of the quadratic function $f(\mathbf{x}) = \frac{1}{2} \mathbf{x}^\top A \mathbf{x} - \mathbf{x}^\top \mathbf{b}$ for positive definite matrices (Golub & Van Loan, 2012). This function is minimized with a simple three-term recurrence, where each iteration involves a single MVM with the matrix A .

After n iterations CG is guaranteed to converge to the exact solution $A^{-1} \mathbf{b}$, although in practice numerical convergence depends on the conditioning of A rather than n . Extremely accurate solutions typically require only $k \ll n$ iterations (depending on the conditioning of A) and $k \leq 100$ suffices in most cases (Golub & Van Loan, 2012). For the kernel matrix \widehat{K}_{XX} , the standard running time of linear CG is $\mathcal{O}(kn^2)$ (the time for k MVMs). This runtime, which is already faster than the Cholesky decomposition, can be greatly improved if the kernel matrix K_{XX} affords fast MVMs. Fast MVMs are possible if the data are structured (Cunningham et al., 2008; Saatçi, 2012), or by using a structured inducing point method (Wilson & Nickisch, 2015).

2.2. The Lanczos algorithm

The Lanczos algorithm factorizes a symmetric matrix $A \in \mathbb{R}^{n \times n}$ as QTQ^\top , where $T \in \mathbb{R}^{n \times n}$ is symmetric tridiagonal and $Q \in \mathbb{R}^{n \times n}$ is orthonormal. For a full discussion of the Lanczos algorithm see Golub & Van Loan (2012). Briefly, the Lanczos algorithm uses a probe vector \mathbf{b} and computes an orthogonal basis of the Krylov subspace $\mathcal{K}(A, \mathbf{b})$:

$$\mathcal{K}(A, \mathbf{b}) = \text{span} \{ \mathbf{b}, A\mathbf{b}, A^2\mathbf{b}, \dots, A^{n-1}\mathbf{b} \}.$$

Applying Gram-Schmidt orthogonalization to these vectors produces the vectors of Q , $[\mathbf{b}/\|\mathbf{b}\|, \mathbf{q}_2, \mathbf{q}_3, \dots, \mathbf{q}_n]$ (here $\|\mathbf{b}\|$ is the Euclidean norm of \mathbf{b}). The orthogonalization coefficients are collected into T . Because A is symmetric, each vector needs only be orthogonalized against the two preceding vectors, which results in the tridiagonal structure of T (Golub & Van Loan, 2012). The orthogonalized vectors and coefficients are computed in an iterative manner. k iterations of the algorithm produces the first k orthogonal vectors of $Q_k = [\mathbf{q}_1, \dots, \mathbf{q}_k] \in \mathbb{R}^{n \times k}$ and their corresponding coefficients $T_k \in \mathbb{R}^{k \times k}$. Crucially, k iterations requires only $\mathcal{O}(k)$ matrix vector multiplies with the original matrix A , which is ideal for matrices that afford fast MVMs.

The Lanczos algorithm can be used in the context of GPs for computing log determinants (Dong et al., 2017), and can be used to speed up inference when there is product structure (Gardner et al., 2018). Another application of the Lanczos algorithm is performing matrix solves (Lanczos, 1950; Parlett, 1980; Saad, 1987). Given a symmetric matrix A and a single vector \mathbf{b} , the matrix solve $A^{-1} \mathbf{b}$ is computed by starting the Lanczos algorithm of A with probe vector \mathbf{b} . After k iterations, the solution $A^{-1} \mathbf{b}$ can be approximated

Table 1. Asymptotic complexities of predictive (co)variances (n training points, m inducing points, k Lanczos/CG iterations) and sampling from the predictive distribution (s samples, t test points).

Method	Pre-computation		Computing variances (time)	Drawing s samples (time)
	(time)	(storage)		
Standard GP	$\mathcal{O}(n^3)$	$\mathcal{O}(n^2)$	$\mathcal{O}(n^2)$	$\mathcal{O}(tn^2 + t^2(n+s) + t^3)$
SGPR	$\mathcal{O}(nm^2)$	$\mathcal{O}(m^2)$	$\mathcal{O}(m^2)$	$\mathcal{O}(tm^2 + t^2(m+s) + t^3)$
KISS-GP	–	–	$\mathcal{O}(k(n+m \log m))$	$\mathcal{O}(kt(n+m \log m) + t^2(m+s) + t^3)$
KISS-GP (w/ LOVE)	$\mathcal{O}(k(n+m \log m))$	$\mathcal{O}(km)$	$\mathcal{O}(k)$	$\mathcal{O}(ks(t+m))$

using the computed Lanczos factors Q_k and T_k as

$$A^{-1}\mathbf{b} \approx \|\mathbf{b}\|Q_k T_k^{-1}\mathbf{e}_1, \quad (3)$$

where \mathbf{e}_1 is the unit vector $[1, 0, 0, \dots, 0]$. In fact, the linear CG algorithm can be derived from (3) when A is positive definite (Golub & Van Loan, 2012). Linear CG tends to be preferred for matrix solves in practice, since Lanczos solves require storing the $Q_k \in \mathbb{R}^{n \times k}$ matrix. However, one advantage of Lanczos is that the Q_k and T_k matrices can be used to jump-start subsequent matrix solves $A^{-1}\mathbf{b}'$. Parlett (1980), Saad (1987), Schneider & Willsky (2001), and Nickisch et al. (2009) argue that subsequent solves can be approximated as

$$A^{-1}\mathbf{b}' \approx Q_k T_k^{-1} Q_k^\top \mathbf{b}'. \quad (4)$$

2.3. Kernel Interpolation for Scalable Structured GPs

Structured kernel interpolation (SKI) (Wilson & Nickisch, 2015) is an inducing point method explicitly designed for fast MVM-based inference. Given a set of m inducing points, $U = [\mathbf{u}_1, \dots, \mathbf{u}_m]$, SKI assumes that a data point \mathbf{x} can be well-approximated as a *local interpolation* of U . For example, using cubic interpolation (Keys, 1981), \mathbf{x} is expressed in terms of its 4 closest inducing points, and the interpolation weights are captured in a sparse vector $\mathbf{w}_\mathbf{x}$. The $\mathbf{w}_\mathbf{x}$ interpolation vectors are used to approximate the kernel matrix $K_{XX} \approx \tilde{K}_{XX}$:

$$\tilde{K}_{XX} = W_X^\top K_{UU} W_X. \quad (5)$$

Here, $W_X = [\mathbf{w}_{\mathbf{x}_1}, \dots, \mathbf{w}_{\mathbf{x}_n}]$ contains the interpolation vectors for all \mathbf{x}_i , and K_{UU} is the covariance matrix between inducing points. MVMs with \tilde{K}_{XX} (i.e. $W_X^\top K_{UU} W_X \mathbf{v}$) require at most $\mathcal{O}(n + m^2)$ time due to the $\mathcal{O}(n)$ sparsity of W_X . Wilson & Nickisch (2015) reduce this runtime even further with *Kernel Interpolation for Scalable Structured GPs* (KISS-GP), an instantiation of their SKI approach in which all inducing points U lie on a regularly spaced grid. This gives K_{UU} Toeplitz structure (or Kronecker and Toeplitz structure), resulting in the ability to perform MVMs in at most $\mathcal{O}(n + m \log m)$ time.

Computing predictive means. One advantage of KISS-GP’s fast MVMs is the ability to perform constant time

predictive mean calculations (Wilson & Nickisch, 2015; Wilson et al., 2015). Substituting the KISS-GP approximate kernel into (1) (and assuming a prior mean of 0 for brevity), the predictive mean is given by

$$\mu_{f|\mathcal{D}}(\mathbf{x}^*) = \mathbf{w}_{\mathbf{x}^*}^\top \underbrace{K_{UU} W_X (W_X^\top K_{UU} W_X + \sigma^2 I)^{-1} \mathbf{y}}_{\mathbf{a}}. \quad (6)$$

Because $\mathbf{w}_{\mathbf{x}^*}$ is the only term in (6) that depends on \mathbf{x}^* , the remainder of the equation (denoted as \mathbf{a}) is pre-computed and $\mu_{f|\mathcal{D}}(\mathbf{x}^*) = \mathbf{w}_{\mathbf{x}^*}^\top \mathbf{a}$ (Throughout this paper blue will highlight computations that do not depend on test data). This pre-computation takes $\mathcal{O}(n + m \log m)$ time using linear CG (Wilson et al., 2015). After computing and caching \mathbf{a} , the multiplication $\mathbf{w}_{\mathbf{x}^*}^\top \mathbf{a}$ requires $\mathcal{O}(1)$ time, as $\mathbf{w}_{\mathbf{x}^*}$ has only four nonzero elements.

3. Lanczos Variance Estimates (LOVE)

In this section we introduce LOVE, an approach to efficiently approximate the predictive covariance

$$k_{f|\mathcal{D}}(\mathbf{x}_i^*, \mathbf{x}_j^*) = k_{\mathbf{x}_i^* \mathbf{x}_j^*} - \mathbf{k}_{X\mathbf{x}_i^*}^\top (K_{XX} + \sigma^2 I)^{-1} \mathbf{k}_{X\mathbf{x}_j^*},$$

where $X^* = [\mathbf{x}_1^*, \dots, \mathbf{x}_t^*]$ denotes a set of t test points, and $X = [\mathbf{x}_1, \dots, \mathbf{x}_n]$ a set of n training points.

Solving $(K_{XX} + \sigma^2 I)^{-1}$ naïvely scales $\mathcal{O}(n^3)$, but is typically done as a one-time pre-computation during training since K_{XX} does not depend on the test data. At test time, all covariance calculations cost $\mathcal{O}(n^2)$. In what follows, we will gradually build a significantly faster method for computing predictive covariances, mirroring the *pre-compute phase* and *test phase* structure of the naïve approach.

3.1. A first $\mathcal{O}(m^2)$ approach with KISS-GP

It is possible to obtain some computational savings when using inducing point methods. For example, we can replace $\mathbf{k}_{X\mathbf{x}_i^*}$ and K_{XX} with their corresponding KISS-GP approximations, $\tilde{\mathbf{k}}_{X\mathbf{x}_i^*}$ and \tilde{K}_{XX} , which we restate here:

$$\tilde{\mathbf{k}}_{X\mathbf{x}_i^*} = W_X^\top K_{UU} \mathbf{w}_{\mathbf{x}_i^*}, \quad \tilde{K}_{XX} = W_X^\top K_{UU} W_X.$$

W_X is the sparse interpolation matrix for training points X ; $\mathbf{w}_{\mathbf{x}_i^*}$ and $\mathbf{w}_{\mathbf{x}_j^*}$ are the sparse interpolations for \mathbf{x}_i^* and

\mathbf{x}_j^* respectively. Substituting these into (2) results in the following approximation to the predictive covariance:

$$k_{f|\mathcal{D}}(\mathbf{x}_i^*, \mathbf{x}_j^*) \approx k_{\mathbf{x}_i^* \mathbf{x}_j^*} - \tilde{\mathbf{k}}_{XX}^\top (\tilde{K}_{XX} + \sigma^2 I)^{-1} \tilde{\mathbf{k}}_{X\mathbf{x}_j^*}. \quad (7)$$

By fully expanding the second term in (7), we obtain

$$\mathbf{w}_{\mathbf{x}_i^*}^\top \underbrace{K_{UU} W_X (\tilde{K}_{XX} + \sigma^2 I)^{-1} W_X^\top K_{UU}}_{\mathbf{C}} \mathbf{w}_{\mathbf{x}_j^*} \quad (8)$$

Precomputation phase. Denote by \mathbf{C} the braced portion of (8). Critically, \mathbf{C} neither depends on test point \mathbf{x}_i^* nor \mathbf{x}_j^* and we can pre-compute it offline during training. The predictive covariance calculation becomes:

$$k_{f|\mathcal{D}}(\mathbf{x}_i^*, \mathbf{x}_j^*) \approx k_{\mathbf{x}_i^* \mathbf{x}_j^*} - \mathbf{w}_{\mathbf{x}_i^*}^\top \mathbf{C} \mathbf{w}_{\mathbf{x}_j^*} \quad (9)$$

Computing \mathbf{C} requires m linear solves with $\tilde{K}_{XX} = (W_X^\top K_{UU} W_X + \sigma^2 I)$: one for each column vector in $W_X^\top K_{UU}$. Computing the right hand sides takes $\mathcal{O}(nm)$ time total because W_X^\top is an $n \times m$ matrix with four non-zero elements per row. Because \tilde{K}_{XX} is exactly the data matrix used in KISS-GP, each of these solves takes $\mathcal{O}(n + m \log m)$ time (Wilson & Nickisch, 2015) and we can solve all m systems in $\mathcal{O}(mn + m^2 \log m)$ time.

Test phase. As \mathbf{w}_i^* contains only four nonzero elements, the inner product of \mathbf{w}_i^* with a vector takes $\mathcal{O}(1)$ time, and the multiplication $\mathbf{w}_i^{*\top} \mathbf{C}$ requires $\mathcal{O}(m)$ time during testing.

Limitations. Although this technique offers computational savings over non-inducing point methods, the quadratic dependence on m in the pre-computation phase is a limiting computational bottleneck. In contrast, all other operations with KISS-GP require at most linear storage and near-linear time. Indeed, one of the hallmarks of KISS-GP is the ability to use a very large number of inducing points $m = \Theta(n)$ so that kernel computations are nearly exact.

In practice, it is often preferred to avoid this pre-computation phase due to its quadratic dependence on m . Instead, (7) is computed directly using linear CG to compute the matrix solve. This has a cost of $\mathcal{O}(kn + km \log m)$, which is the time to perform k iterations of linear CG with \tilde{K}_{XX} . The dependence on n and m is problematic in the common case of large training sets or many inducing points.

3.2. Fast predictive (co-)variances with LOVE

We propose to overcome this limitation through an altered pre-computation step. In particular, we approximate \mathbf{C} in (9) as a low rank matrix. Letting \mathbf{R} and \mathbf{R}' be $k \times m$ matrices such that $\mathbf{R}^\top \mathbf{R}' \approx \mathbf{C}$, we rewrite (9) as:

$$k_{f|\mathcal{D}}(\mathbf{x}_i^*, \mathbf{x}_j^*) \approx k_{\mathbf{x}_i^* \mathbf{x}_j^*} - (\mathbf{R} \mathbf{w}_i^*)^\top \mathbf{R}' \mathbf{w}_j^*, \quad (10)$$

which reduces the complexity to $\mathcal{O}(k)$, due to the sparsity of $\mathbf{w}_{\mathbf{x}_i^*}$ and $\mathbf{w}_{\mathbf{x}_j^*}$. Recalling the approximation $(\tilde{K}_{XX} +$

$\sigma^2 I)^{-1} \mathbf{b} \approx Q_k T_k^{-1} Q_k^\top \mathbf{b}$ from Section 2.2, we substitute in the Lanczos approximation to the definition for \mathbf{C} and derive forms for \mathbf{R} and \mathbf{R}' :

$$\begin{aligned} \mathbf{C} &= K_{UU} W_X \underbrace{(\tilde{K}_{XX} + \sigma^2 I)^{-1}}_{\text{Apply Lanczos}} W_X^\top K_{UU} \\ &\approx K_{UU} W_X (Q_k T_k^{-1} Q_k^\top) W_X^\top K_{UU} \\ &= \underbrace{K_{UU} W_X Q_k}_{\mathbf{R}^\top} \underbrace{T_k^{-1} Q_k^\top W_X^\top K_{UU}}_{\mathbf{R}'} \end{aligned}$$

To compute \mathbf{R} and \mathbf{R}' in an efficient manner, we compute k iterations of the Lanczos algorithm to achieve $(\tilde{K}_{XX} + \sigma^2 I) \approx Q_k T_k Q_k^\top$ using the average column vector $\mathbf{b} = \frac{1}{m} W_X^\top K_{UU} \mathbf{1}$ as a probe vector. Both \mathbf{R} and \mathbf{R}' are $m \times k$ matrices, and thus require $\mathcal{O}(mk)$ storage.

Computing \mathbf{R} . To compute \mathbf{R} , we first multiply $W_X Q_k$. Since W_X is sparse, this takes $\mathcal{O}(nk)$ time, and results in a $\mathcal{O}(m \times k)$ matrix. Next we multiply K_{UU} by the result. Since K_{UU} is Toeplitz, each MVM takes $\mathcal{O}(m \log m)$ time, and there are k of them. The total running time to compute \mathbf{R} is therefore $\mathcal{O}(kn + km \log m)$.

Computing \mathbf{R}' . To compute \mathbf{R}' , we note that $\mathbf{R}' = T_k^{-1} \mathbf{R}^\top$. We can perform this solve by Cholesky decomposing T , which is positive definite since \tilde{K}_{XX} is. The decomposition take $\mathcal{O}(m)$ time and each of the k solves similarly takes $\mathcal{O}(m)$ time because T is tridiagonal (Loan, 1999).

After this $\mathcal{O}(kn + km \log m)$ total pre-computation, all predictive variances can be computed in $\mathcal{O}(k)$ time using (10). k depends on the conditioning of the matrix and not its size (Golub & Van Loan, 2012). In practice, a constant $k \leq 100$ is sufficient for most matrices (Golub & Van Loan, 2012), and therefore k can be considered to be constant. Running times are summarized in Table 1.

3.3. Predictive distribution sampling with LOVE

A distinctive property of LOVE is that it allows us not only to efficiently compute predictive variances, but also predictive *covariances*, and operations involving the predictive covariance matrix. Let $X^* = [\mathbf{x}_1^*, \dots, \mathbf{x}_t^*]$ be a test set of t points. In many applications (2) will be used only to compute the predictive variance terms for each \mathbf{x}_i^* , i.e. $k_{f|\mathcal{D}}(\mathbf{x}_i^*, \mathbf{x}_i^*)$. However if we want to draw samples from $\mathbf{f}^* | \mathcal{D}$ — the predictive function evaluated on $\mathbf{x}_1^*, \dots, \mathbf{x}_t^*$, then we must evaluate the cross-covariance terms as well. Sampling functions from the posterior is an operation that arises commonly when using Gaussian processes. In Bayesian optimization, it is a necessary step in several popular acquisition functions such as predictive entropy search (Hernández-Lobato et al., 2014), max-value entropy search (Wang & Jegelka, 2017), and the knowledge gradient (Frazier et al., 2009). There are many other applications where GP sampling could be useful; however,

parametric approximations are often used instead due to the large asymptotic cost of sampling (Deisenroth & Rasmussen, 2011).

The predictive distribution $\mathbf{f}^* | \mathcal{D}$ is multivariate normal with mean $\mu_{f|\mathcal{D}}(X^*) \in \mathbb{R}^t$ and covariance $k_{f|\mathcal{D}}(X^*, X^*) \in \mathbb{R}^{t \times t}$. We can draw a sample from $\mathbf{f}^* | \mathcal{D}$ by first sampling Gaussian noise $\mathbf{v} \sim \mathcal{N}(0, I^{t \times t})$ and reparameterizing:

$$\mu_{f|\mathcal{D}}(X^*) + S\mathbf{v}, \quad (11)$$

where S is a matrix such that $SS^\top = k_{f|\mathcal{D}}(X^*, X^*)$. Typically S is taken to be the factor from the Cholesky decomposition of $k_{f|\mathcal{D}}(X^*, X^*)$. Computing the Cholesky decomposition incurs a $\mathcal{O}(t^3)$ cost on top of the $\mathcal{O}(t^2)$ predictive covariance evaluations. This may be prohibitively expensive, even with constant-time predictive covariances.

A Fast Low-Rank Sampling Matrix. We use LOVE and KISS-GP to rewrite (10) as

$$\begin{aligned} k_{f|\mathcal{D}}(X^*, X^*) &\approx W_{X^*}^\top K_{UU} W_{X^*} - (R W_{X^*})^\top (R' W_{X^*}) \\ &= W_{X^*}^\top (K_{UU} - R^\top R') W_{X^*}. \end{aligned} \quad (12)$$

where $W_{X^*} = [\mathbf{w}_{x_1^*}, \dots, \mathbf{w}_{x_n^*}]$ is the interpolation matrix for test points. Once again we have reduced the full covariance matrix to a test-independent term that can be pre-computed. Directly computing $K_{UU} - R^\top R'$ would result in $\mathcal{O}(m^2)$ time and space complexity. Therefore, we apply the Lanczos algorithm once again in the pre-computation phase to obtain a rank- k approximation:

$$K_{UU} - R^\top R' \approx Q_k' T_k' Q_k'^\top. \quad (13)$$

This Lanczos decomposition requires k matrix vector multiplies with $K_{UU} - R^\top R'$, each of which requires $\mathcal{O}(m \log m)$ time. Substituting (13) into (12), we get:

$$k_{f|\mathcal{D}}(X^*, X^*) = W_{X^*}^\top Q_k' T_k' Q_k'^\top W_{X^*}. \quad (14)$$

If we take the Cholesky decomposition of $T_k' = LL^\top$ (a $\mathcal{O}(k)$ operation since T_k' is tridiagonal), we rewrite (14) as

$$k_{f|\mathcal{D}}(X^*, X^*) \approx W_{X^*}^\top \underbrace{Q_k' LL^\top Q_k'}_{\substack{S \\ S^\top}} W_{X^*}. \quad (15)$$

Setting $S = Q_k' L T_k$, we see that $k_{f|\mathcal{D}}(X^*, X^*) = (W_{X^*}^\top S)(W_{X^*}^\top S)^\top$. $S \in \mathbb{R}^{m \times k}$ can be precomputed and cached since it does not depend on test data. In total, this pre-computation takes $\mathcal{O}(km \log m + mk^2)$ time in addition to what is required for fast variances. To sample from the predictive distribution, we need to evaluate (11), which involves multiplying $W_{X^*}^\top S \mathbf{v}$. Multiplying \mathbf{v} by S requires $\mathcal{O}(mk)$ time, and finally multiplying by $W_{X^*}^\top$ takes $\mathcal{O}(tk)$ time. Therefore, drawing s samples (corresponding to s different values of \mathbf{v}) takes $\mathcal{O}(sk(t+m))$ time total during the testing phase (see Table 1). Note that alternative approaches have a *cubic* dependence on t , whereas this approach has a *linear* dependence on t .

Algorithm 1: LOVE for fast predictive variances.

Input : $\mathbf{w}_{x_i^*}, \mathbf{w}_{x_j^*}$ – interpolation vectors for $\mathbf{x}_i^*, \mathbf{x}_j^*$
 $k_{\mathbf{x}_i^*, \mathbf{x}_j^*}$ – prior covariance between $\mathbf{x}_i^*, \mathbf{x}_j^*$
 $\mathbf{b} = \frac{1}{m} W_X^\top K_{UU} \mathbf{1}$ – average column of $W_X^\top K_{UU}$
 $\text{mvm_K}_{XX}()$: a function that performs MVMs with $(W_X^\top K_{UU} W_X + \sigma^2 I) \approx \widehat{K}_{XX}$
 $\text{mvm_K}_{UX}()$: a function that performs MVMs with $(K_{UU} W_X) \approx K_{UX}$
Output : Approximate predictive variance $k_{f|\mathcal{D}}(\mathbf{x}_i^*, \mathbf{x}_j^*)$.

if R, R' have not previously been computed **then**

```

     $Q_k, T_k \leftarrow \text{lanczos}_k(\text{mvm\_K}_{XX}, \mathbf{b})$ 
    // k iter. of Lanczos w/
    // matrix  $\widehat{K}_{XX}$  and probe vec.  $\mathbf{b}$ 
     $L_{T_k} \leftarrow \text{cholesky\_factor}(T_k)$ 
     $R \leftarrow (\text{mvm\_K}_{UX}(Q_k))^\top$ ; //  $R = Q_k^\top W_X^\top K_{UU}$ 
     $R' \leftarrow \text{cholesky\_solve}(R, L_{T_k})$ 
    //  $R' = T_k^{-1} Q_k^\top W_X^\top K_{UU}$ 

```

end

```

 $\mathbf{u} \leftarrow \text{sparse\_mm}(R, \mathbf{w}_{x_i^*})$ 

```

```

 $\mathbf{v} \leftarrow \text{sparse\_mm}(R', \mathbf{w}_{x_j^*})$ 

```

```

return  $k_{\mathbf{x}_i^*, \mathbf{x}_j^*} - \mathbf{u}^\top \mathbf{v}$ 

```

3.4. Extension to additive kernel compositions

LOVE is applicable even when the KISS-GP approximation is used with an additive composition of kernels,

$$\tilde{k}(\mathbf{x}_i, \mathbf{x}_j) = \mathbf{w}_{\mathbf{x}_i}^{(1)\top} K_{UU}^{(1)} \mathbf{w}_{\mathbf{x}_j}^{(1)} + \dots + \mathbf{w}_{\mathbf{x}_i}^{(d)\top} K_{UU}^{(d)} \mathbf{w}_{\mathbf{x}_j}^{(d)}.$$

Additive structure has recently been a focus in several Bayesian optimization settings as it causes the cumulative regret to depend only linearly on the number of dimensions (Kandasamy et al., 2015; Wang et al., 2017; Gardner et al., 2017; Wang & Jegelka, 2017). Additionally, deep kernel learning models (Wilson et al., 2016a;b) typically use kernels that are sums of one-dimensional kernel functions applied to each deep network feature. To apply LOVE, we note that this additive composition can be re-written as

$$\tilde{k}(\mathbf{x}_i, \mathbf{x}_j) = \begin{bmatrix} \mathbf{w}_{\mathbf{x}_i}^{(1)} \\ \vdots \\ \mathbf{w}_{\mathbf{x}_i}^{(d)} \end{bmatrix}^\top \begin{bmatrix} K_{UU}^{(1)} & \dots & 0 \\ \vdots & \ddots & \vdots \\ 0 & \dots & K_{UU}^{(d)} \end{bmatrix} \begin{bmatrix} \mathbf{w}_{\mathbf{x}_j}^{(1)} \\ \vdots \\ \mathbf{w}_{\mathbf{x}_j}^{(d)} \end{bmatrix}. \quad (16)$$

The block matrices in (16) are analogs of their 1-dimensional counterparts in (5). Therefore, we can directly apply Algorithm 1, replacing W_X , $\mathbf{w}_{x_i^*}$, $\mathbf{w}_{x_j^*}$, and K_{UU} with their block forms. The block \mathbf{w} vectors are $\mathcal{O}(d)$ -sparse, and therefore interpolation takes $\mathcal{O}(d)$ time. MVMs with the block K_{UU} matrix take $\mathcal{O}(dm \log m)$ time by exploiting the block-diagonal structure. With d additive components, predictive variance computations cost only a factor $\mathcal{O}(d)$ more than their 1-dimensional counterparts.

4. Results

In this section we demonstrate the effectiveness of LOVE, both at computing predictive variances and also at sampling from predictive distributions. When using LOVE we use $k = 50$ Lanczos iterations. All KISS-GP models use $m = 10,000$ inducing points unless otherwise stated. We implement LOVE and all KISS-GP models with the GPyTorch library¹. All experiments utilize GPU acceleration. Timing results are performed on an NVIDIA GTX 1080.

4.1. Predictive Variances

In these experiments, we aim to measure the accuracy and speed of LOVE at computing predictive variances with KISS-GP models. To measure accuracy, we train a single KISS-GP model, and compute the variances with LOVE and without LOVE (i.e. standard variance computations). We then compare how well the LOVE variances compare to standard (non-LOVE) variances, which are exact and can therefore be taken as ground truth. We report the scaled mean absolute error (SMAE)² (Rasmussen & Williams, 2006) of the LOVE variances as measured against the standard variances. (Note that the predictive posterior means are *completely identical* with both methods, as LOVE only affects variance calculations.) In order to control for variations during training, we use the same GP model for both variance computations and only vary the prediction procedure.

One-dimensional example. We first demonstrate LOVE on a complex one-dimensional regression task. The airline passenger dataset (**Airline**) measures the average monthly number of passengers from 1949 to 1961 (Hyndman, 2005). We aim to extrapolate the numbers for the final 4 years (48 measurements) given data for the first 8 years (96 measurements). Accurate extrapolation on this dataset requires a kernel function capable of expressing various patterns, such as the spectral mixture (SM) kernel (Wilson & Adams, 2013). Our goal is to evaluate if LOVE produces reliable predictive variances, even with complex kernel functions.

We train a KISS-GP model with a 10-mixture SM kernel, and compute the model’s predicted variances with and without LOVE. In Figure 1, we see that the confidence intervals from both computations agree almost everywhere. The SMAE of LOVE’s predicted variances (compared with the non-LOVE variances) is 1.29×10^{-4} . Although not shown in the plot, we confirm the reliability of these predictions by computing the log-likelihood of the test data. We compare the KISS-GP model (with and without LOVE) to an exact GP and a sparse variational GP (SGPR) model³ (Titsias, 2009; Hensman et al., 2013). All methods achieve nearly

¹ github.com/cornellius-gp/gpytorch

² Mean absolute error divided by the variance of y .

³ Implemented in GPFlow (Matthews et al., 2017), $m = 1000$.

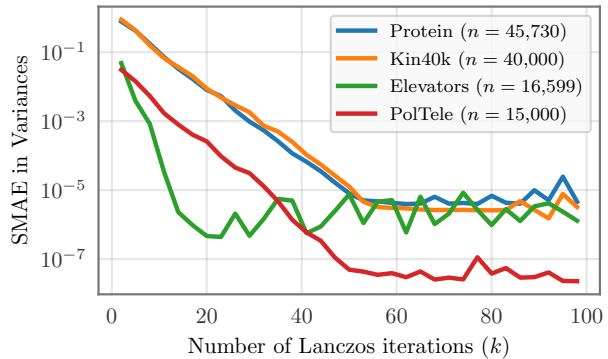


Figure 2. Predictive variance error as a function of the Lanczos iterations (KISS-GP model, $m = 10,000$, Protein, Kin40k, PolTele, Elevators UCI datasets).

identical log-likelihoods, ranging from -221 to -222 .

Speedup on large datasets. We measure the speed of computing predictive variances with LOVE for the entire test set on several large-scale regression benchmarks from the UCI repository (Asuncion & Newman, 2007). For each of the datasets, we train a KISS-GP model with deep kernel learning (DKL/KISS-GP) using the architectures described in (Wilson et al., 2016b). We compare the speed of computing the DKL/KISS-GP model’s predictive variances with LOVE and without LOVE. In addition, we compare against the speed of SGPR, one of the leading approaches to scalable GPs. The SGPR model uses a standard RBF kernel and $m = 1000$ inducing points. On all datasets, we measure the time to compute variances **from scratch** (i.e. assuming we have not pre-computed any terms) and the time to compute variances **after pre-computing** any terms that aren’t specific to test points. (Note that the KISS-GP benchmark without LOVE does not pre-compute any terms.)

Table 2 summarizes the results. We see that KISS-GP with LOVE yields a substantial speedup over KISS-GP without LOVE and SGPR across all datasets. The speedup is between $4\times$ and $44\times$ when computing variances from scratch and *up to* $2,000\times$ after pre-computation. The biggest improvements are obtained on the largest datasets, since the running time of LOVE is independent of dataset size after pre-computation, unlike the other methods. It is worth noting that these speedups come with *almost no loss in accuracy*. In the last column of Table 2, we report the SMAE of LOVE variances from the KISS-GP model, as compared against the standard variances (without LOVE). On all datasets, we find that the scaled mean average error of this approximation is on the order of 10^{-5} or less.

Accuracy vs. Lanczos iterations. In Figure 2, we measure the SMAE of LOVE’s predictive variances as a function of the number of Lanczos iterations (k). We train a DKL/KISS-GP model with a 4-layer deep RBF kernel and 10,000 inducing points on the four largest datasets from Table 2. We

Table 2. Speedup and accuracy of KISS-GP with LOVE for computing predictive variances. For KISS-GP, all results reported use deep kernel learning. All models utilize GPU acceleration. (n is the number of data points, d is the data dimensionality.) The scaled mean average error (SMAE) is measured by comparing the variance computations of a KISS-GP model with and without LOVE.

Dataset			Speedup over KISS-GP (w/o LOVE)		Speedup over SGPR		Variance SMAE (compared to KISS-GP w/o LOVE)
Name	n	d	(from scratch)	(after pre-comp.)	(from scratch)	(after pre-comp.)	
Airfoil	1,503	6	4×	84×	9×	183×	1.30×10^{-5}
Skillcraft	3,338	19	25×	167×	17×	110×	2.00×10^{-7}
Parkinsons	5,875	20	46×	443×	16×	152×	8.80×10^{-5}
PoleTele	15,000	26	78×	1178×	21×	343×	2.90×10^{-5}
Elevators	16,599	18	64×	1017×	20×	316×	1.20×10^{-6}
Kin40k	40,000	8	31×	2065×	12×	798×	3.90×10^{-7}
Protein	45,730	9	44×	1151×	20×	520×	5.30×10^{-5}

Table 3. Accuracy and computation time of drawing samples from the predictive distribution.

Dataset	Sample Covariance Error			Speedup over Standard GP w/ Cholesky			
	Standard GP w/ Cholesky	Fourier Features	KISS-GP w/ LOVE	Standard GP w/ Cholesky	Fourier Features	KISS-GP w/ LOVE (from scratch)	KISS-GP w/ LOVE (after pre-comp.)
PolTele	8.8×10^{-4}	1.8×10^{-3}	7.5×10^{-4}	1×	22×	21×	881×
Elevators	2.6×10^{-7}	3.1×10^{-4}	5.5×10^{-7}	1×	31×	25×	1062×
BayesOpt (Eggholder)	7.7×10^{-4}	1.5×10^{-3}	8.0×10^{-5}	1×	16×	19×	775×
BayesOpt (Styblinski-Tang)	5.4×10^{-4}	7.3×10^{-3}	5.2×10^{-4}	1×	11×	42×	18,100×

measure the relative mean average error of LOVE’s predictive variances compared to the standard KISS-GP variances. As seen in Figure 2, error decreases *exponentially* with the number of Lanczos iterations, up until roughly 50 iterations. After roughly 50 iterations, the error levels off, though this may be an artifact of floating-point precision (which may also cause small subsequent fluctuations). Recall that number of Lanczos iterations (k) corresponds with the rank of the R and R' matrices in (10).

4.2. Sampling

We evaluate the quality of posterior samples drawn as described in Section 3.3. We compare these samples to those drawn from an **exact GP**, and to samples drawn with random **Fourier features** (Rahimi & Recht, 2008), a baseline described in both (Wang & Jegelka, 2017) and (Hernández-Lobato et al., 2014). We use 5000 random Fourier features, which was the maximum number of features that could be used without exhausting available GPU memory. To control for variations during training, we learn hyperparameters on the simple GP and then use the same hyperparameters for the all methods.

We test on the two largest UCI datasets which can still be solved exactly (PolTele, Elevators) and two Bayesian optimization benchmark functions after 100 iterations

(Eggholder – 2 dimensional, and Styblinski-Tang – 10 dimensional). On the two UCI datasets, we use the same DKL architecture as in the previous section. We use a standard (non-deep) RBF kernel for Eggholder BayesOpt. For Syblinski-Tang, we exploit the function’s inherent additive structure and use the additive kernel decomposition suggested by Kandasamy et al. (2015).⁴

Sample accuracy. In Table 3 we evaluate the accuracy of the different sampling methods. We draw $s = 1000$ samples at $t = 10,000$ test locations and compare the sample covariance matrix with the true posterior covariance matrix $k_{f|\mathcal{D}}(X^*, X^{*'})$ in terms of element-wise mean absolute error. It is worth noting that all methods incur some error – even the Cholesky method which computes an “exact” sampling matrix. Nevertheless, both Cholesky and LOVE produce very accurate sample covariance matrices. Both methods achieve between 1 and 3 orders of magnitude less error than the random Fourier Feature method. Though LOVE and Cholesky are comparable in terms of accuracy, LOVE is significantly faster. Even without pre-computation (i.e. sampling “from scratch”), LOVE is comparable to the Fourier features method in terms of speed. After pre-computation, LOVE is up to 18,000 times faster.

⁴ The Syblinski-Tang KISS-GP model uses the sum of 10 RBF kernels – one for each dimension – and $m = 100$ inducing points.

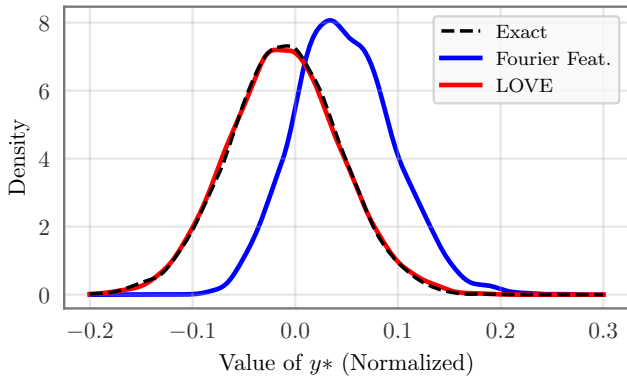


Figure 3. A density estimation plot of the predictive maximum distribution, $p(y^* | \mathcal{D})$ for the (normalized) Eggholder function after 100 iterations of BayesOpt. Samples drawn with LOVE closely match samples drawn using a Cholesky decomposition (Exact). See Wang & Jegelka (2017) for details.

Bayesian optimization. Many acquisition functions in Bayesian optimization rely on sampling from the posterior GP. For example, max-value entropy search (Wang & Jegelka, 2017) draws samples from a posterior GP in order to estimate the function’s maximum value $p(y^* | \mathcal{D})$. The corresponding maximum *location* distribution, $p(x^* | \mathcal{D})$, is also the primary distribution of interest in predictive entropy search (Hernández-Lobato et al., 2014).

In Figure 3, we test how faithful each sampling method is to the true distribution $p(y^* | \mathcal{D})$ on the Eggholder benchmark. We plot kernel density estimates of the sampled maximum value distributions after 100 iterations of BayesOpt. Since the Cholesky method computes an “exact” sampling matrix, its sampled max-value distribution can be considered closest to ground truth. The Fourier feature sampled distribution differs significantly. In contrast, LOVE’s sampled distribution very closely resembles the “exact” Cholesky distribution. However, LOVE is 700× faster than the exact Cholesky method on this dataset (Table 3).

5. Discussion, Related Work, and Conclusion

This paper has primarily focused on KISS-GP as an underlying inducing point method due to its near constant asymptotic complexities when used with LOVE. However, LOVE and MVM inference are fully compatible with other inducing point techniques as well. Many inducing point methods make use of the subset of regressors (SOR) kernel approximation $K_{XX} \approx K_{XU}K_{UU}^{-1}K_{UX}$, optionally with a diagonal correction (Snelson & Ghahramani, 2006), and focus on the problem of learning the inducing point locations (Quiñero-Candela & Rasmussen, 2005; Titsias, 2009). After $\mathcal{O}(m^3)$ work to Cholesky decompose $\mathcal{O}(K_{UU})$, this approximate kernel affords $\mathcal{O}(n + m^2)$ MVMs. One could apply LOVE to these methods and compute a test-invariant cache in $\mathcal{O}(knm + km^2)$ time, and then compute single

predictive covariances in $\mathcal{O}(mk)$ time. We note that, since these inducing point methods by construction make a rank m approximation to the kernel, setting $k = m$ results in the Lanczos decomposition being exact, and recovers exactly the $\mathcal{O}(nm^2)$ precomputation time and $\mathcal{O}(m^2)$ prediction time of these methods.

Ensuring Lanczos solves are accurate. Given a matrix \widehat{K}_{XX} , the Lanczos decomposition $Q_k T_k Q_k^\top$ is designed to approximate the solve $\widehat{K}_{XX}^{-1} \mathbf{b}$, where \mathbf{b} is the first column of Q_k . As argued in Section 2.2, the Q_k and T_k can usually be re-used to approximate the solves $\widehat{K}_{XX}^{-1} (W_X^\top K_{UU}) \approx Q_k T_k^{-1} Q_k^\top (W_X^\top K_{UU})$. This property of the Lanczos decomposition is why LOVE can compute fast predictive variances. While this method usually produces accurate solves, the solves will not be accurate if some columns of $(W_X^\top K_{UU})$ are (nearly) orthogonal to the columns of Q_k . In this scenario, Saad (1987) suggests that the additional Lanczos iterations with a new probe vector will correct these errors. In practice, we find that these countermeasures are almost never necessary with LOVE – the Lanczos solves are almost always accurate.

Numerical stability of Lanczos. A practical concern for LOVE is round-off errors that may affect the Lanczos algorithm. In particular it is common in floating point arithmetic for the vectors of Q to lose orthogonality (Paige, 1970; Simon, 1984; Golub & Van Loan, 2012), resulting in an incorrect decomposition. To correct for this, several methods such as full reorthogonalization and partial or selective reorthogonalization exist (Golub & Van Loan, 2012). In our implementation, we use full reorthogonalization when a loss of orthogonality is detected. In practice, the cost of this correction is absorbed by the parallel performance of the GPU due to the small value of k and does not impact the final running time.

Conclusion. In this paper, we have demonstrated a method for computing predictive covariances and drawing samples from the predictive distribution in nearly constant time with almost no loss in accuracy. Whereas the running times of previous state-of-the-art methods depend on dataset size, LOVE provides *constant time* predictive variances. In addition to providing scalable predictions, LOVE’s fast sampling procedure has the potential to dramatically simplify a variety of applications of Gaussian processes. Many applications require both posterior samples and speed (Deisenroth & Rasmussen, 2011; Hernández-Lobato et al., 2014; Wang & Jegelka, 2017). As sampling has traditionally scaled cubically with the number of test points, many methods have resorted to parametric approximations or finite basis approaches to approximate sampling efficiently. Because LOVE produces reliable posterior samples with minimal overhead, it may render these approaches unnecessary. The ability to obtain samples in linear time may unlock new applications for Gaussian Processes in the future.

Acknowledgements

JRG, GP, and KQW are supported in part by the III-1618134, III1526012, and IIS-1149882 grants from the National Science Foundation, as well as the Bill and Melinda Gates Foundation and the Office of Naval Research. AGW is supported by NSF IIS-1563887.

References

- Asuncion, Arthur and Newman, David. Uci machine learning repository. <https://archive.ics.uci.edu/ml/>, 2007. Last accessed: 2018-02-05.
- Cunningham, John P, Shenoy, Krishna V, and Sahani, Maneesh. Fast gaussian process methods for point process intensity estimation. In *ICML*, pp. 192–199. ACM, 2008.
- Deisenroth, Marc and Rasmussen, Carl E. Pilco: A model-based and data-efficient approach to policy search. In *ICML*, pp. 465–472, 2011.
- Deisenroth, Marc Peter, Fox, Dieter, and Rasmussen, Carl Edward. Gaussian processes for data-efficient learning in robotics and control. *IEEE Transactions on Pattern Analysis and Machine Intelligence*, 37(2):408–423, 2015.
- Dong, Kun, Eriksson, David, Nickisch, Hannes, Bindel, David, and Wilson, Andrew Gordon. Scalable log determinants for gaussian process kernel learning. In *NIPS*, 2017.
- Doshi-Velez, Finale and Kim, Been. A roadmap for a rigorous science of interpretability. *arXiv preprint arXiv:1702.08608*, 2017.
- Frazier, Peter, Powell, Warren, and Dayanik, Savas. The knowledge-gradient policy for correlated normal beliefs. *INFORMS journal on Computing*, 21(4):599–613, 2009.
- Gardner, Jacob, Guo, Chuan, Weinberger, Kilian, Garnett, Roman, and Grosse, Roger. Discovering and exploiting additive structure for bayesian optimization. In *AISTATS*, pp. 1311–1319, 2017.
- Gardner, Jacob R., Pleiss, Geoff, Wu, Ruihan, Weinberger, Kilian Q., and Wilson, Andrew Gordon. Product kernel interpolation for scalable gaussian processes. In *AISTATS*, 2018.
- Golub, Gene H and Van Loan, Charles F. *Matrix computations*, volume 3. JHU Press, 2012.
- Hensman, James, Fusi, Nicolo, and Lawrence, Neil D. Gaussian processes for big data. *arXiv preprint arXiv:1309.6835*, 2013.
- Hernández-Lobato, José Miguel, Hoffman, Matthew W, and Ghahramani, Zoubin. Predictive entropy search for efficient global optimization of black-box functions. In *NIPS*, pp. 918–926, 2014.
- Hyndman, Rob J. Time series data library. <http://www-personal.buseco.monash.edu.au/~hyndman/TSDL/>, 2005. Last accessed: 2018-02-05.
- Kandasamy, Kirthevasan, Schneider, Jeff, and Póczos, Barnabás. High dimensional bayesian optimisation and bandits via additive models. In *International Conference on Machine Learning*, pp. 295–304, 2015.
- Keys, Robert. Cubic convolution interpolation for digital image processing. *IEEE transactions on acoustics, speech, and signal processing*, 29(6):1153–1160, 1981.
- Lanczos, Cornelius. *An iteration method for the solution of the eigenvalue problem of linear differential and integral operators*. United States Governm. Press Office Los Angeles, CA, 1950.
- Loan, Charles F Van. *Introduction to scientific computing: a matrix-vector approach using MATLAB*. Prentice Hall PTR, 1999.
- Matthews, Alexander G de G, van der Wilk, Mark, Nickson, Tom, Fujii, Keisuke, Boukouvalas, Alexis, León-Villagrà, Pablo, Ghahramani, Zoubin, and Hensman, James. Gpflow: A gaussian process library using tensorflow. *Journal of Machine Learning Research*, 18(40): 1–6, 2017.
- Nickisch, Hannes, Pohmann, Rolf, Schölkopf, Bernhard, and Seeger, Matthias. Bayesian experimental design of magnetic resonance imaging sequences. In *Advances in Neural Information Processing Systems*, pp. 1441–1448, 2009.
- Paige, CC. Practical use of the symmetric lanczos process with re-orthogonalization. *BIT Numerical Mathematics*, 10(2):183–195, 1970.
- Parlett, Beresford N. A new look at the lanczos algorithm for solving symmetric systems of linear equations. *Linear algebra and its applications*, 29:323–346, 1980.
- Quiñonero-Candela, Joaquin and Rasmussen, Carl Edward. A unifying view of sparse approximate gaussian process regression. *Journal of Machine Learning Research*, 6 (Dec):1939–1959, 2005.
- Rahimi, Ali and Recht, Benjamin. Random features for large-scale kernel machines. In *Advances in neural information processing systems*, pp. 1177–1184, 2008.

- Rasmussen, Carl Edward and Williams, Christopher KI. *Gaussian processes for machine learning*, volume 1. MIT press Cambridge, 2006.
- Saad, Youcef. On the lanczos method for solving symmetric linear systems with several right-hand sides. *Mathematics of computation*, 48(178):651–662, 1987.
- Saatçi, Yunus. *Scalable inference for structured Gaussian process models*. PhD thesis, University of Cambridge, 2012.
- Schneider, Michael K and Willsky, Alan S. Krylov subspace estimation. *SIAM Journal on Scientific Computing*, 22(5):1840–1864, 2001.
- Schulam, Peter and Saria, Suchi. What-if reasoning with counterfactual gaussian processes. In *NIPS*, 2017.
- Simon, Horst D. The lanczos algorithm with partial re-orthogonalization. *Mathematics of Computation*, 42(165):115–142, 1984.
- Snelson, Edward and Ghahramani, Zoubin. Sparse Gaussian processes using pseudo-inputs. In *NIPS*, pp. 1257–1264, 2006.
- Snoek, Jasper, Larochelle, Hugo, and Adams, Ryan P. Practical bayesian optimization of machine learning algorithms. In *Advances in neural information processing systems*, pp. 2951–2959, 2012.
- Titsias, Michalis K. Variational learning of inducing variables in sparse gaussian processes. In *AISTATS*, pp. 567–574, 2009.
- Wang, Zi and Jegelka, Stefanie. Max-value entropy search for efficient bayesian optimization. In *ICML*, 2017.
- Wang, Zi, Li, Chengtao, Jegelka, Stefanie, and Kohli, Pushmeet. Batched high-dimensional bayesian optimization via structural kernel learning. *arXiv preprint arXiv:1703.01973*, 2017.
- Wilson, Andrew and Adams, Ryan. Gaussian process kernels for pattern discovery and extrapolation. In *ICML*, pp. 1067–1075, 2013.
- Wilson, Andrew G, Hu, Zhiting, Salakhutdinov, Ruslan R, and Xing, Eric P. Stochastic variational deep kernel learning. In *Advances in Neural Information Processing Systems*, pp. 2586–2594, 2016a.
- Wilson, Andrew Gordon and Nickisch, Hannes. Kernel interpolation for scalable structured gaussian processes (kiss-gp). In *ICML*, pp. 1775–1784, 2015.
- Wilson, Andrew Gordon, Dann, Christoph, and Nickisch, Hannes. Thoughts on massively scalable gaussian processes. *arXiv preprint arXiv:1511.01870*, 2015.
- Wilson, Andrew Gordon, Hu, Zhiting, Salakhutdinov, Ruslan, and Xing, Eric P. Deep kernel learning. In *AISTATS*, pp. 370–378, 2016b.
- Zhou, Jianlong, Arshad, Syed Z, Luo, Simon, and Chen, Fang. Effects of uncertainty and cognitive load on user trust in predictive decision making. In *IFIP Conference on Human-Computer Interaction*, pp. 23–39. Springer, 2017.